Journal of Groundwater Science and Engineering Vol.9 No.3: 256—268

Journal homepage: http://gwse.iheg.org.cn

Identification of suitable sites for open and bore well using ground magnetic survey

A Muthamilselvan*

Assistant Professor, Department of Remote Sensing, Bharathidasan University, Trichy-23.

Abstract: The study aims to identify a suitable site for open and bore well in a farmhouseusing ground magnetic survey in south India. It also aims to define depth to granitoid and structural elements which traverse the selected area. Magnetic data (n=84) measured, processed and interpreted as qualitative and quantitatively. The results of total magnetic intensities indicate that the area is composed of linear magnetic lows trending NE-SW direction and circular to semi-circular causative bodies. The magnetic values ranged from −137 nT to 2 345 nT with a mean of 465 nT. Reduction to equator shows significant shifting of causative bodies in the southern and northern directions. Analytical signal map shows exact boundary of granitic bodies. Cosine directional filter has brought out structural element trending NE-SW direction. Results of individual profile brought to light structurally weak zone between 90 m and 100 m in all the profile lines. Sudden decrease of magnetic values from 2 042 nT to 126 nT noticed in profile line 6 between 20 m and 30 m indicates fault occurrence. Magnetic breaks obtained from these maps were visualized, interpreted and identified two suitable sites for open and bore well. Radially averaged power spectrum estimates depth of shallow and deep sources in 5 m and 50 m, respectively. Euler method has also been applied to estimate depth of granitoid and structural elements using structural indexes 0, 1, 2, and 3 and found depth ranges from <10 m to >90 m. Study indicates magnetic method is one of the geophysical methods suitable for groundwater exploration and site selection for open and borewells.

Keywords: Magnetic method; Groundwater exploration; Euler deconvolution; Open well

Received: 09 Nov 2020/ Accepted: 03 May 2021

Introduction

Different geophysical methods like electrical, electromagnetic, gravity and magnetic are regularly used to identify subsurface structures, groundwater and minerals. Magnetic survey depends on the magnetic properties of the material being surveyed. The intensity of magnetization varies with respect to the magnetic susceptibility of the material concerned. It is also used to locate and define the extent of sedimentary basins where the basement rocks are brought near the surface, which is structural high, magnetic anomalies are large and characterized by strong relief. On the other hand, low magnetic values for deep sedimentary basin produce contour with and gentle gradient of magnetic maps (Adagunodo et al. 2015). Magnetic method is also used to delineate magnetic field intensity in an area underlain by different lithologies with varying magnetic mineral contents (Dransfield et al. 2018). Magnetic method also gives information about depth to the basement rocks (Danielet al. 2018). Magnetic survey used to locate groundwater potential zone (Sultan et al. 2015) and spatial confirmation of existing fault/lineaments (Muthamilselvan et al. 2017). According to Hansen et al. (2005), magnetic methods are widely used in almost all areas of near-surface geophysics. In some subfields, such as buried ordnance detection, magnetic methods are particularly important. The geophysical method such a magnetic is the primary exploration tool in the search for minerals. In other areas, the magnetic method has evolved from its sole use for mapping basement structure to a wide range of new applications, such as locating intrasedimentary

*Corresponding author: A Muthamilselvan, *E-mail address*: thamil1978@gmail.com

DOI: 10.19637/j.cnki.2305-7068.2021.03.008

Muthamilselvan A. 2021. Identification of suitable sites for open and bore well using ground magnetic survey. Journal of Groundwater Science and Engineering, 9(3): 256-268.

faults, defining subtle lithologic contacts, mapping salt domes in weakly magnetic sediments, and better defining targets through 3D inversion (Nabighian et al. 2005).

The main aim of the present study is to explore the groundwater potentiality to locate the positions of open and bore wells in a farmhouse. To achieve the goals, the ground magnetic method has been used as effective geophysical tools in this study. Geophysical techniques were not only used for the direct detection of groundwater occurrences but also helped to estimate the aquifer parameters, groundwater quality and movement, saline water intrusions and buried valleys (UNESCO, 1998). Besides, geophysics can also screen potential drilling locations, decreasing the risk of drilling in unproductive areas (Tsiboah, 2002).

1 Study area

The study area taken up for magnetic survey belongs to hard rock terrain located in the Perambalur district of Tamil Nadu. Lithologically, the study area belongs to Archaean rocks which include hornblende biotite gneiss intruded by younger granites (Fig. 1). However, the farm taken up for the study is totally covered by granites/ weathered granites and alluvium. Major landuse pattern includes crop and fallow land, with few pockets of barren rocky outcrop noticed. Fractures trending NE-SW, NW-SW and E-W directions were recorded from the open wells.

2 Results and discussions

2.1 Magnetic data preprocessing and analysis

Magnetic data have been collected using Proton Precession Magnetometer over an area of 16 800 km^2. Totally, 84 magnetic data were collected along six profile lines (Fig. 2, Table 1) with sampling interval of 10 m (140 m Length) and 20 m (120 m Width) profile intervals. Diurnal corrections were applied using base station data collected hourly and it was interpolated to the field timing using geosoft software. After removing the diurnal variation from field data, the magnetic data were contoured (Fig. 3) and prepared total magnetic intensity map, regional, residual, reduction to equator and analytical signal maps. All maps were produced on WGS84 ellipsoidal datum with Geographic lat-long projection. Interpretations were made from these maps and identified structural elements traversing in the study area which is used to map the suitable sites for open and bore wells in the agricultural field.

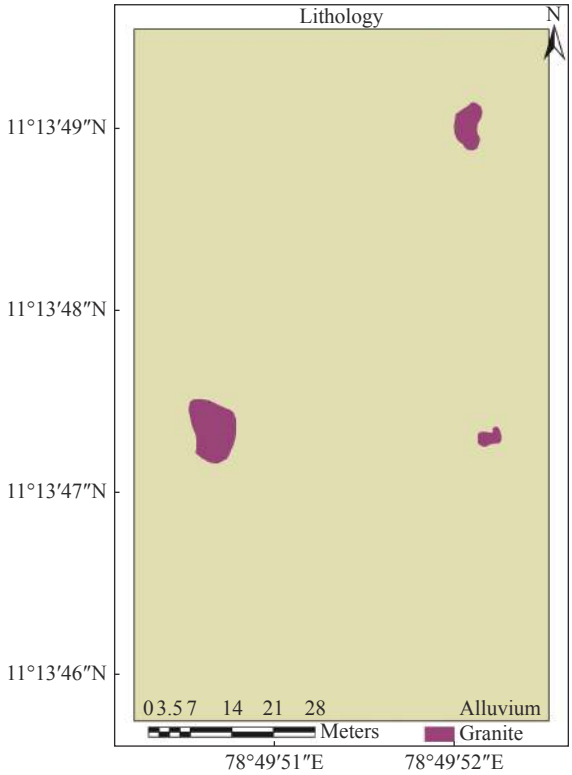

Fig. 1 Lithology of the study area

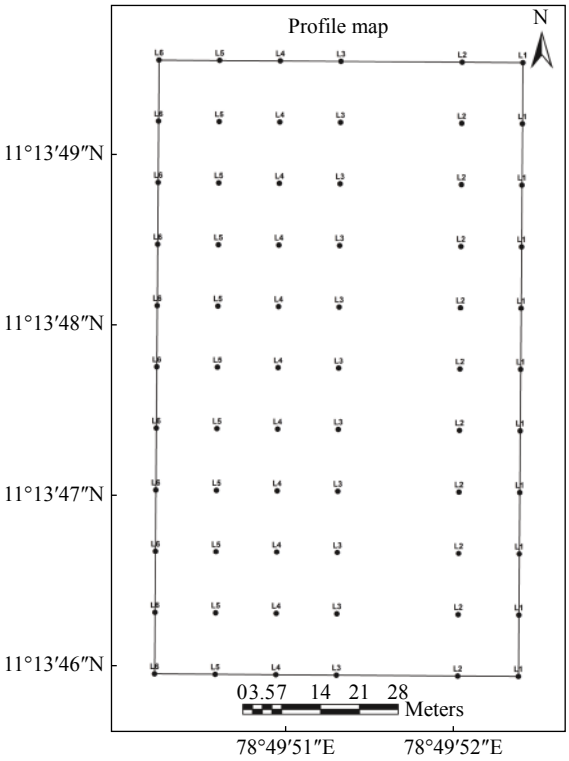

Fig. 2 Profile lines

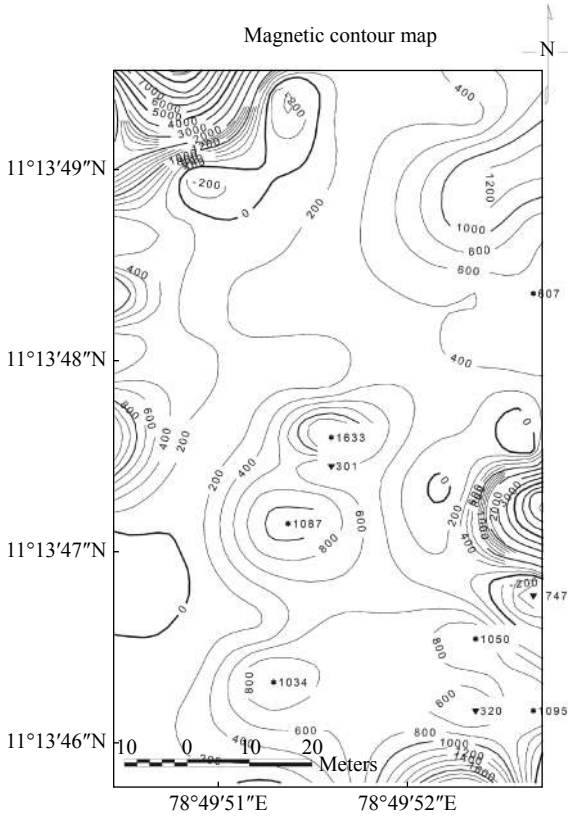

Fig. 3 Magnetic contour

2.2 Total magnetic intensity map

The total magnetic intensity map (TMI) (Fig. 4) indicates that the southern and north eastern part of the study area consists of high magnetic intensities, while the northern and northwestern parts are represented by low magnetic values. The total magnetic values range from −137 nT to 2 345 nT with the mean of 465 nT. The magnetic fields due to magnetized subsurface geological bodies are indistinct due to inclination and declination of the ambient geomagnetic field. This makes it very difficult to estimate the correct shape, size and locations of the causative bodies. To overcome this issue, a reduction to magnetic equator (RTE) filter was applied a modified version of reduction to pole (Grant and Dodds, 1972). The study area is located in state of Tamil Nadu, India, which is closer to the magnetic equator than to the poles and found along lower latitudes around 11°. During this process, the anomalies tend to be shifted horizontally instead of being vertically above their actual locations due to the effect of magnetic inclination. The RTE grid ideally displays the same frequency distribution as the original TMI grid. It also retains geological strike and dips information while removing the effect of magnetization direction. Therefore, it should be equally possible to map structures, divide the region into geologic terrains in the study area. Total magnetic intensity reduced to equator shows significant shifting of causative bodies in the southern and northern direction (Fig. 5). Circular to semi-circular magnetic high anomaly noticed in the study area indicates the presence of granitic bodies. It is also emphasized few subsurface structural features which dissect the study area trending NE-SW and NW-SE directions.

2.3 Analytical signal

The analytical signal amplitude was calculated from the total magnetic intensity which results in the shape of the analytical signal is expected to be centered above the magnetic body. Nabighian (1972) has introduced the concept of the analytic signal for magnetic interpretation and showed that its amplitude yields a bell-shaped function over each corner of a 2D body. Further, the analytical signal of total magnetic intensity (Macleod et al. 1993) is vertically independent of the magnetic inclination of magnetization. Compared to the reduction to pole, analytical signal shows better control for the interpretation of magnetic anomalies in the middle and low altitudes and demarcates the causative bodies more accurately. The analytic signal amplitude over the study area ranges from 4 nT to 766 nT. As a result, circular to semi-circular causative bodies with higher analytic signal values were properly demarcated in the central and southern part of the map (Fig. 6).

The Analytic Signal grid enhances the effect of shallow sources, widens anomalies and almost completely removes the effect of magnetization direction, geological strike and geological dip. Hence, it is difficult and harder to delineate geological structures from the analytical signal map. However, it shows structural elements trending NE-SW direction which was also noticed in the RTE and TMI map.

2.4 Cosine directional filter

It is a spectral domain grid filter which rejects or retains the components of the observed data oriented along with the user specified azimuth. As compared to conventional directional filters, Directional Cosine Filter (DCF) creates a smooth curve in Roll of Range to prevent shorter wave length (Serguel and Jhon, 2000).

DCF was applied to the total magnetic intensities to enhance the structural elements trending in the NE-SW direction. To extract NE-SW linear features, 45° azimuth directions have been used with degree of cosine function as 2. The result of

Table 1 Magnetic data of the study area

S.No	Profile line	Longitude	Latitude	Magnetic Data (nT)			
				Filed	Reading time	Base value	Corrected value
1	L1	78.8313	11.2295	41 399	11.2	41 399.00	0
2	L1	78.8313	11.2296	41 154	11.21	41 398.93	245
3	L1	78.8313	11.2296	40 164	11.22	41 398.85	1 235
4	L1	78.8313	11.2297	41 371	11.23	41 398.78	28
5	L1	78.8313	11.2297	41 338	11.24	41 398.71	61
6	L1	78.8313	11.2298	39 754	11.25	41 398.64	1 645
7	L1	78.8313	11.2298	41 264	11.26	41 398.56	135
8	L1	78.8313	11.2299	41 331	11.27	41 398.49	67
9	L1	78.8313	11.23	40 855	11.28	41 398.42	543
10	L1	78.8313	11.23	40 821	11.29	41 398.35	577
11	L1	78.8313	11.2301	40 770	11.3	41 398.27	628
12	L1	78.8313	11.2302	40 731	11.31	41 398.20	667
13	L1	78.8313	11.2303	40 102	11.32	41 398.13	1 296
14	L1	78.8313	11.2304	40 672	11.33	41 398.05	726
15	L2	78.8311	11.2303	40 814	11.34	41 397.98	584
16	L2	78.8312	11.2303	40 875	11.35	41 397.91	523
17	L2	78.8312	11.2302	41 278	11.36	41 397.84	120
18	L2	78.8312	11.2302	40 361	11.37	41 397.76	1 037
19	L2	78.8312	11.2301	40 215	11.38	41 397.69	1 183
20	L2	78.831	11.23	41 093	11.39	41 397.62	305
21	L2	78.8312	11.23	40 897	11.4	41 397.55	501
22	L2	78.8312	11.2299	41 048	11.41	41 397.47	349
23	L2	78.8312	11.2298	41 226	11.42	41 397.40	171
24	L2	78.8312	11.2298	41 226	11.43	41 397.33	171
25	L2	78.8312	11.2297	41 234	11.44	41 397.25	163
26	L2	78.8312	11.2296	40 213	11.45	41 397.18	1 184
27	L2	78.831	11.2297	41 223	11.46	41 397.11	174
28	L2	78.8311	11.2294	39 336	11.47	41 397.04	2 061
29	L3	78.8313	11.2296	41 007	11.48	41 396.96	390
30	L3	78.8309	11.2295	40 755	11.49	41 396.89	642
31	L3	78.831	11.2296	40 706	11.5	41 396.82	691
32	L3	78.8312	11.2295	40 775	11.51	41 396.75	622
33	L3	78.8312	11.2296	40 405	11.52	41 396.67	992
34	L3	78.831	11.2297	41 455	11.53	41 396.60	−58
35	L3	78.831	11.2298	39 051	11.54	41 396.53	2 346
36	L3	78.831	11.2299	41 332	11.55	41 396.45	64
37	L3	78.831	11.23	41 261	11.56	41 396.38	135
38	L3	78.831	11.2301	41 068	11.57	41 396.31	328
39	L3	78.831	11.2301	41 110	11.58	41 396.24	286
40	L3	78.831	11.2303	41 242	11.59	41 396.16	154
41	L3	78.831	11.2302	41 086	12	41 396.09	310
42	L3	78.831	11.2303	41 221	12.01	41 396.02	175
43	L4	78.8309	11.2303	41 193	12.02	41 395.95	203
44	L4	78.8309	11.2303	41 332	12.03	41 395.87	64
45	L4	78.8309	11.2302	41 284	12.04	41 395.80	112

continued Table1

S.No	Profile line	Longitude	Latitude	Magnetic Data (nT)			
				Filed	Reading time	Base value	Corrected value
46	L4	78.8309	11.2301	41 269	12.05	41 395.73	127
47	L4	78.8309	11.2301	40 994	12.06	41 395.65	402
48	L4	78.8309	11.23	41 307	12.07	41 395.58	89
49	L4	78.8309	11.2299	41 107	12.08	41 395.51	289
50	L4	78.8309	11.2298	40 507	12.09	41 395.44	888
51	L4	78.8309	11.2298	40 327	12.1	41 395.36	1 068
52	L4	78.8309	11.2297	40 742	12.11	41 395.29	653
53	L4	78.8309	11.2294	41 183	12.12	41 395.22	212
54	L4	78.8308	11.2296	40 249	12.13	41 395.15	1 146
55	L4	78.8308	11.2295	40 555	12.14	41 395.07	840
56	L4	78.8306	11.2294	41 304	12.15	41 395.00	91
57	L5	78.8308	11.2294	41 237	12.25	41 394.86	158
58	L5	78.8307	11.2295	41 111	12.26	41 394.71	284
59	L5	78.8307	11.2295	41 302	12.27	41 394.57	93
60	L5	78.8307	11.2296	41 289	12.28	41 394.43	105
61	L5	78.8308	11.2297	41 370	12.29	41 394.29	24
62	L5	78.8308	11.2298	41 346	12.3	41 394.14	48
63	L5	78.8308	11.2298	41 284	12.31	41 394.00	110
64	L5	78.8308	11.2299	41 338	12.32	41 393.86	56
65	L5	78.8308	11.23	41 089	12.33	41 393.71	305
66	L5	78.8308	11.2299	41 089	12.34	41 393.57	305
67	L5	78.8308	11.2301	41 354	12.35	41 393.43	39
68	L5	78.8308	11.2302	41 139	12.36	41 393.29	254
69	L5	78.8308	11.2303	41 241	12.37	41 393.14	152
70	L5	78.8308	11.2304	41 379	12.38	41 393.00	14
71	L6	78.8307	11.2304	39 351	12.39	41 392.86	2 042
72	L6	78.8307	11.2303	39 351	12.4	41 392.71	2 042
73	L6	78.8307	11.2302	41 267	12.41	41 392.57	126
74	L6	78.8307	11.2302	41 283	12.42	41 392.43	109
75	L6	78.8307	11.2301	40 230	12.43	41 392.29	1 162
76	L6	78.8307	11.23	41 181	12.44	41 392.14	211
77	L6	78.8307	11.23	41 298	12.45	41 392.00	94
78	L6	78.8307	11.2299	40 090	12.46	41 391.86	1 302
79	L6	78.8306	11.2298	41 051	12.47	41 391.71	341
80	L6	78.8306	11.2297	41 529	12.48	41 391.57	−137
81	L6	78.8306	11.2298	41 336	12.49	41 391.43	55
82	L6	78.8306	11.2296	41 391	12.5	41 391.29	0
83	L6	78.8306	11.2295	41 234	12.51	41 391.14	157
84	L6	78.8307	11.2294	41 348	12.52	41 391.00	43

the directional filter significantly brought out NE-SW structural elements. Linear low magnetic observed from the SW corner to NE corner of the map certainly gives information about the fracture zone trend (Fig. 7). These zones are considered favorable loci for groundwater exploration.

2.5 Regional and residual anomaly

Regional and residual anomaly maps were generated using Gaussian Regional/Residual filters under Geosoft Oasis Montaj environment (Fig. 8 and Fig. 9). It is used to delineate shallow and deep

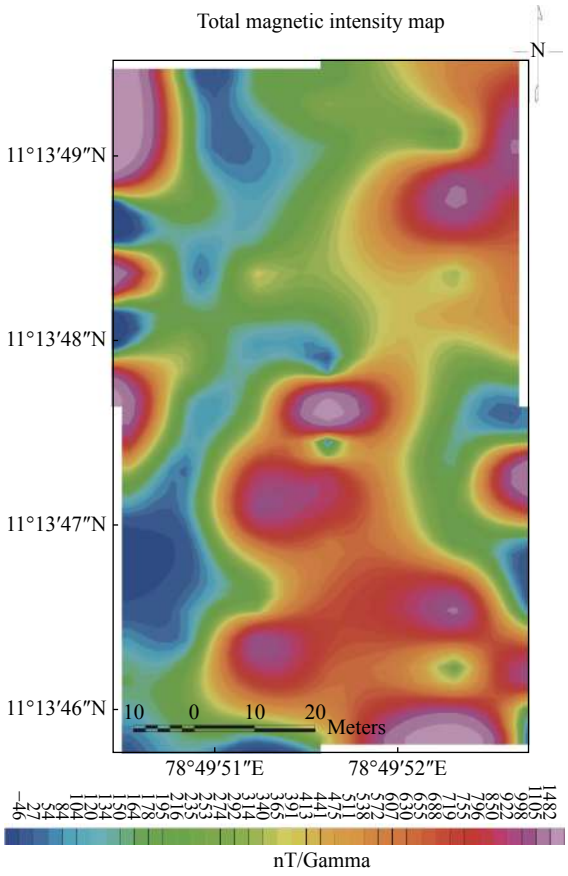

Fig. 4 Total magnetic intensity map

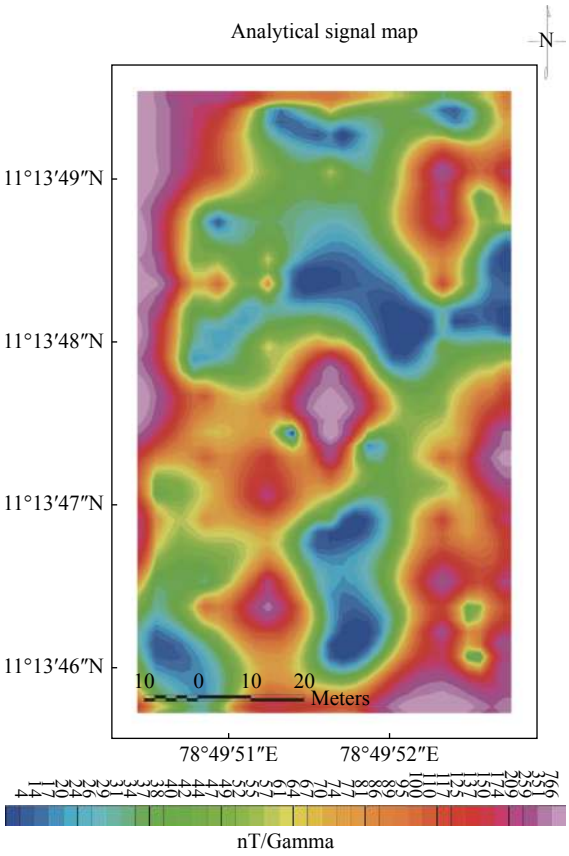

Fig. 6 Analytical signal map

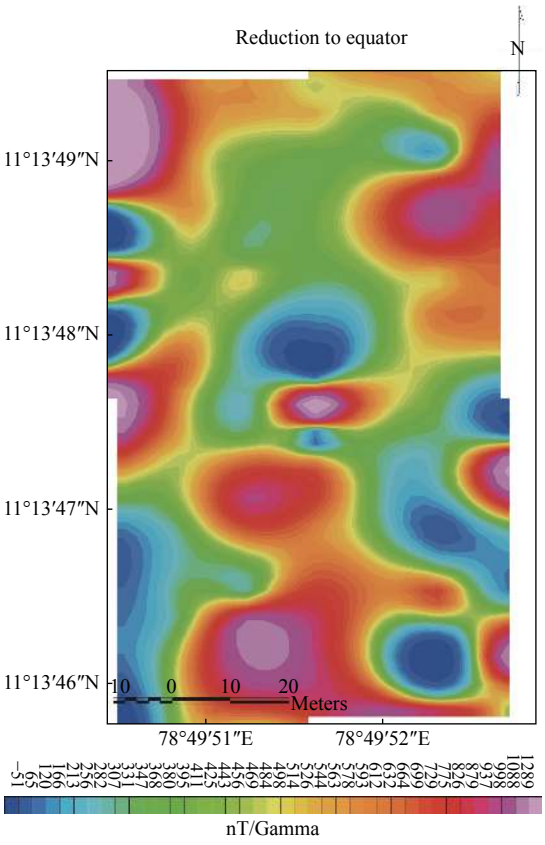

Fig. 5 Reduction to equator map

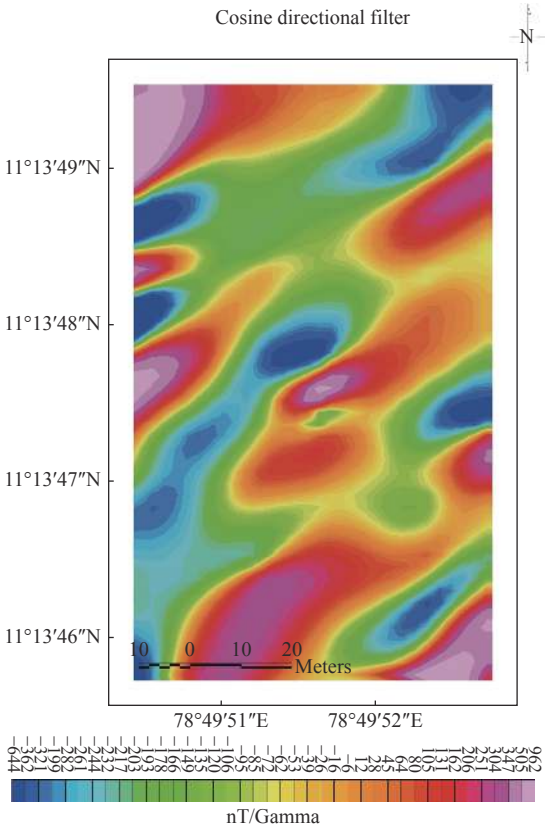

Fig. 7 Cosine directional filter

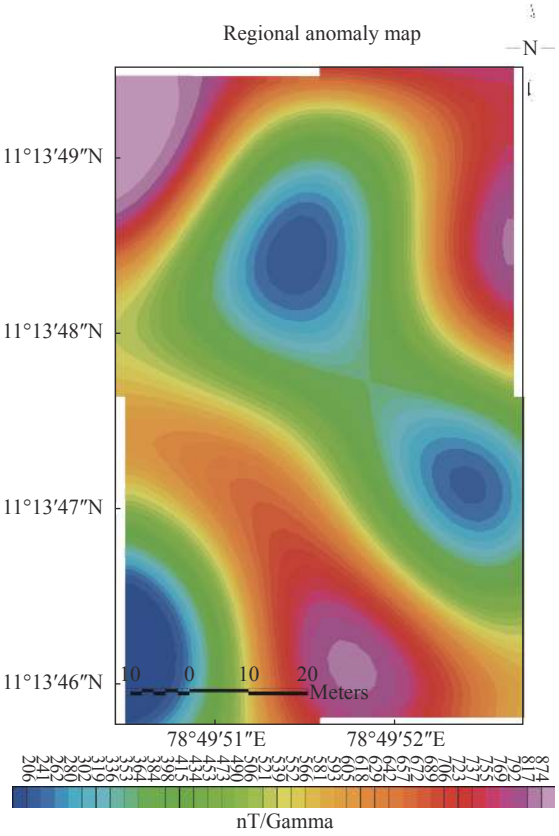

Fig. 8 Regional anomaly map

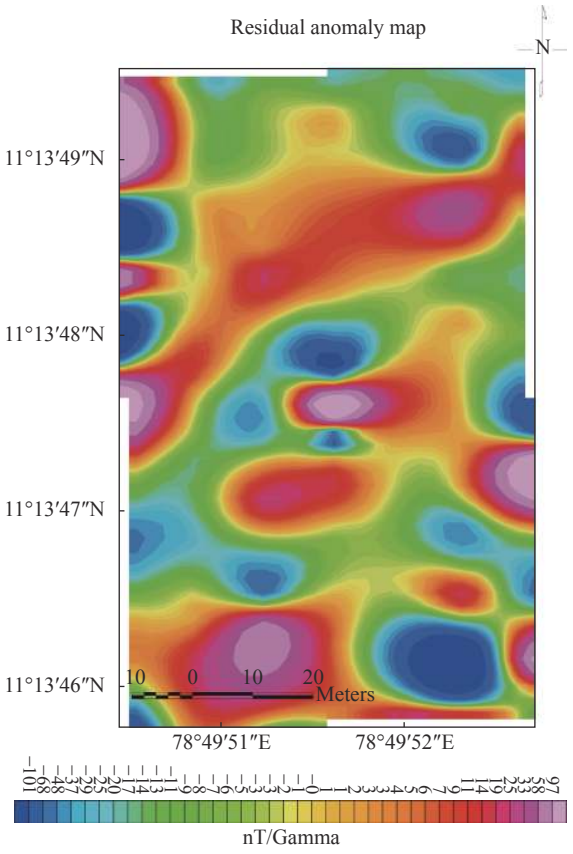

Fig. 9 Residual anomaly map

causative bodies located in the study area. Deep magnetized bodies cause magnetic anomalies with a long spatial wavelength and shallow magnetized bodies cause magnetic anomalies with a short spatial wavelength which is often called regional and residual trends respectively. If the research workers are interested in shallow structures, then the long wavelength anomalies are filtered and considered as noise. Similarly, if the research workers are interested in deeper structure, the short wavelengths are noise and need to be removed.

Cutoff wavelength of 10 000 m^{-1} has been used to create the regional anomaly map which enhanced the deeper causative bodies in the northern and southern part of granites. It indicates that the depth perceptions for those rocks are deep when compared to the other magnetic intensity noticed in the study area. Similarly, depth perceptions of NE-SW trending structural element are deep. In residual anomaly, the cutoff wavelength which is used to create the anomaly map for the study area is 10 000 m^{-1}. The individual causative bodies were separated and shallow features are clearly highlighted. The central and southern parts of the residual image show circular to semi-circular causative bodies (Fig. 9), which exhibit the occurrences of granitic body in shallow depth.

2.6 Identification of suitable sites

The results of interpretation of various maps indicate that the presence of structural elements like shear and fault in the study area (Fig. 9a-Fig. 9f). Magnetic breaks such as fracture noticed in the TMI and RTE have also been encountered in the ASandDCFmaps.Regionalmapshowsthedepthpersistence of those structural elements in the central part of the area trending NW-SE direction. NE-SW curvy linear fracture noticed in the residual map indicates the occurrence of shallow fracture. Based on interpreter knowledge, suitable sites for the open and bore wells have been suggested in the SE corner and central part of the farm show in Fig. 11.

3 Interpretation of magnetic profiles

The results of individual profile interpretation of the magnetic field (Fig. 10a-Fig. 10f) indicate variable anomalies which are an indication of susceptibility contrast of the weathered and massive granites. These show that the causative bodies are not evenly distributed across the study area. Minimum and Maximum values obtained

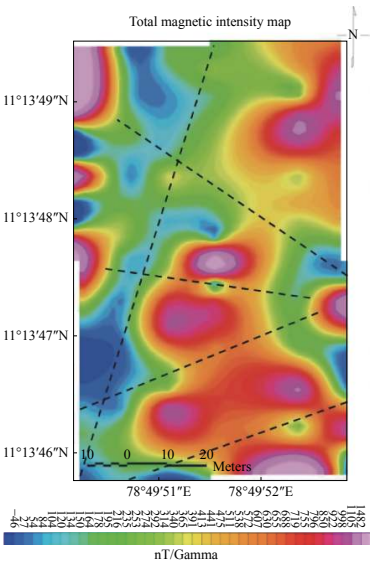

Fig. 9a Manetic breaks from TMI

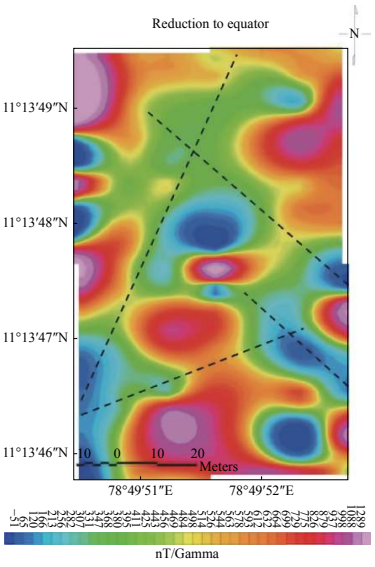

Fig. 9b Manetic breaks from RTE

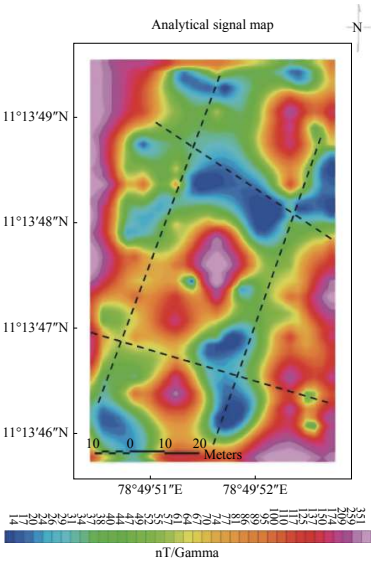

Fig. 9c Manetic breaks from AS

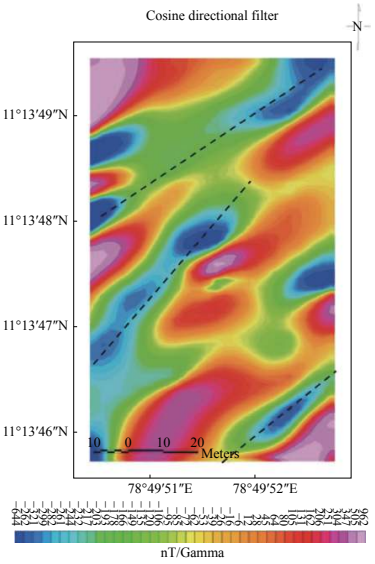

Fig. 9d Manetic breaks from TMI

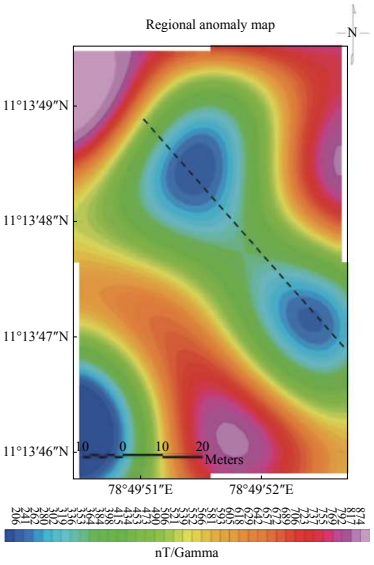

Fig. 9e Manetic breaks from regional

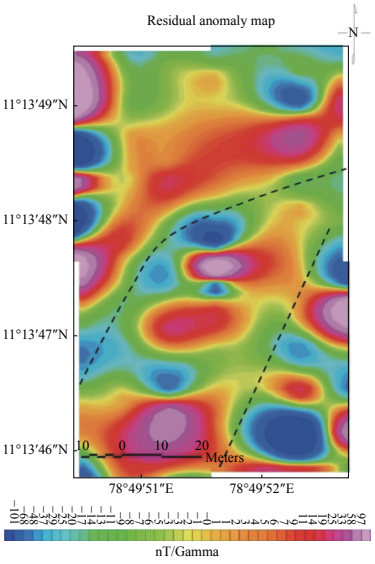

Fig. 9f Manetic breaks from residual

Notes: Dashed lines from all maps represents shear and faults

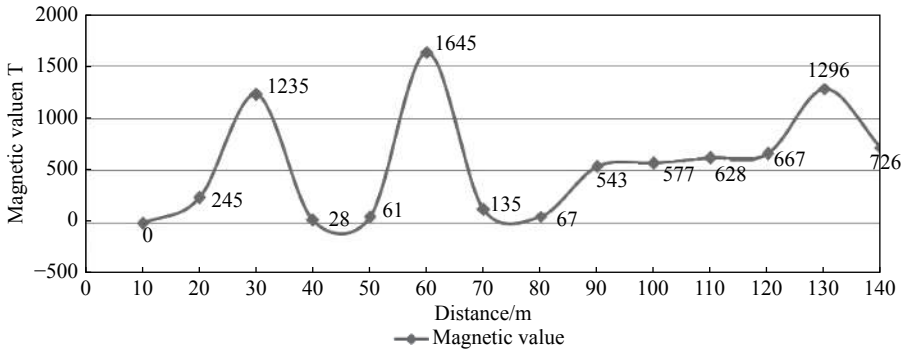

Fig. 10a Magnetic profile line 1

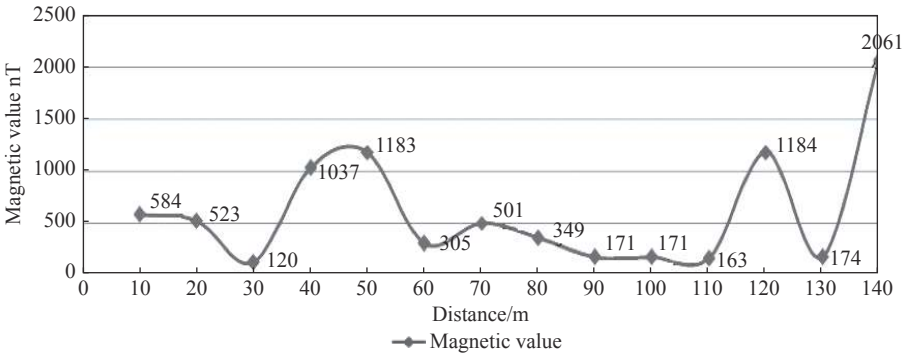

Fig. 10b Magnetic Profile Line 2

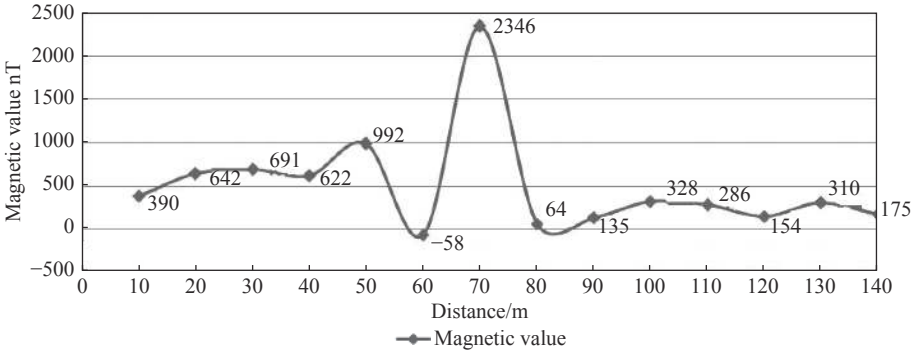

Fig. 10c Magnetic profile line 3

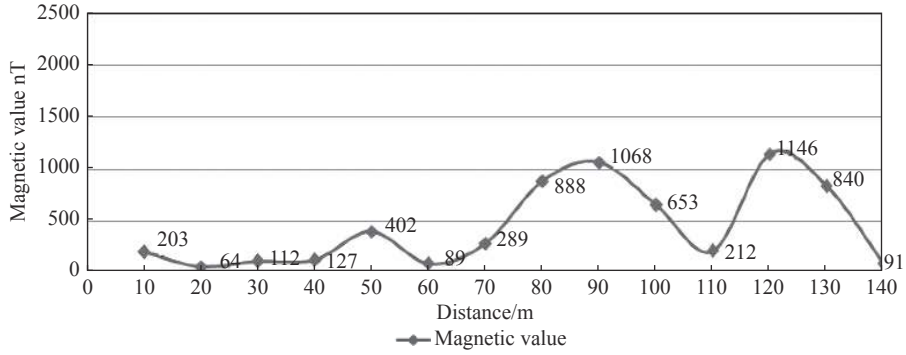

Fig. 10d Magnetic Profile Line 4

along the profile between 1 and 6 shown in Table 2 and Fig. 10a - Fig. 10f. The magnetic anomaly values (between 90 m and 100 m) were observed in decreasing order along profiles suggest possible

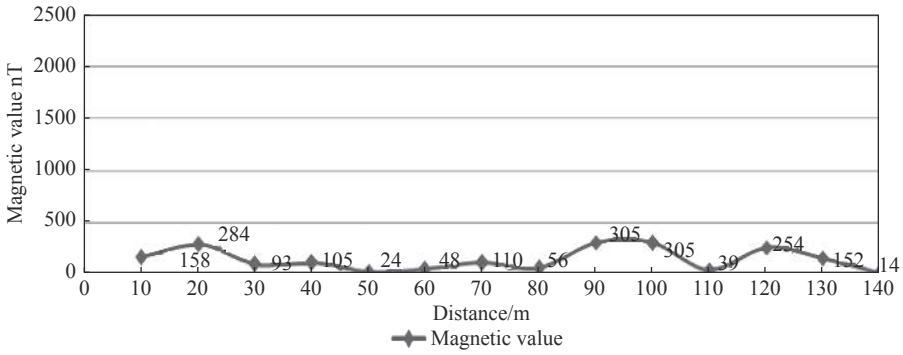

Fig. 10e Magnetic profile line 5

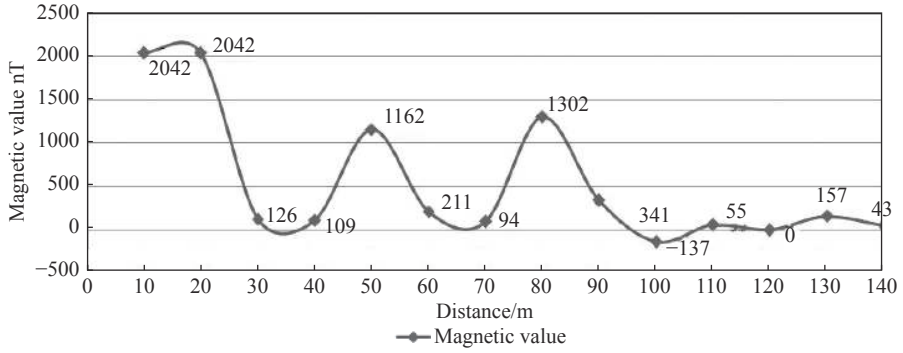

Fig. 10f Magnetic profile line 6

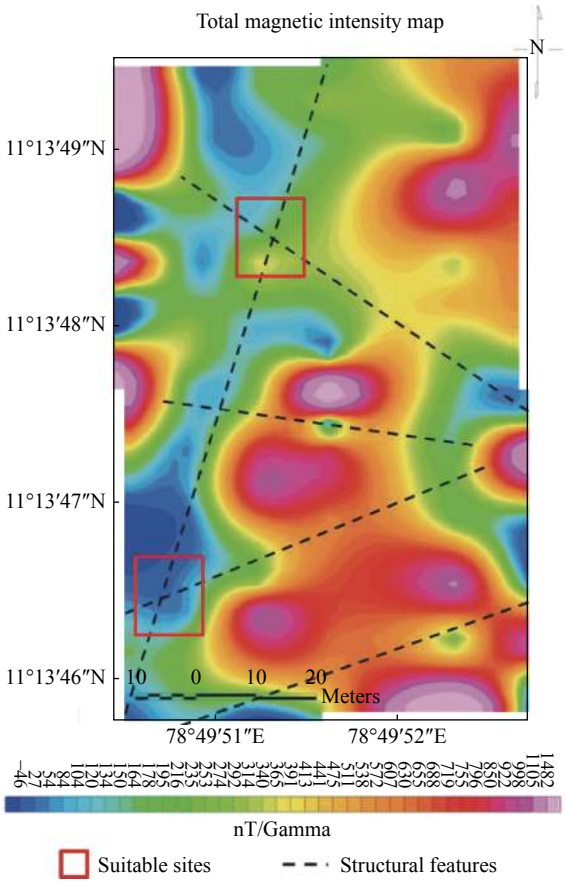

Fig. 11 Suitable sites for open and bore well

Table 2 Magnetic values along the profile lines

Profile	Minimum (nT)	Maximum (nT)
Line 1	0	1 644
Line 2	119	2 061
Line 3	−58	2 345
Line 4	63	1 146
Line 5	14	304
Line 6	−137	2 041

discontinuity in the magnetic basement or faults or fracture zones along these profile lines. Profile line 3 shows bell shaped curve at 70 m indicates the presence of circular high magnetic body. The sudden drop of magnetic values from 2 042 nT to 126 nT in profile no 6 indicates the presence of fracture at this point. Among 6 profile lines, the 5th one shows entirely low magnetic values.

As a result, two locations were proposed for the open and bore well sites in the farmhouse based on the significant information obtained from various magnetic maps and profiles analysis. Site 1 is proposed on the northern side of the map where intersection of magnetic breaks was noticed. Magnetic breaks are nothing but fractures; intersection of these fractures increases the structural

porosity and permeability in hard rock terrain. These zones are considered as good potential zone for groundwater exploration. In addition to that, site 1 also falls between 90 m and 100 m which is interpreted as structurally weak zone. Similarly, site 2 is proposed on the southeastern corner of the map where NE-SW structural elements confirmed with various maps and also sudden decrease of magnetic values from 2 042 nT to 126 nT between 20 m and 30 m indicated presence of fracture/fault along the profile line 6 (Fig. 11).

4 Quantitative analysis

4.1 Radially averaged power spectrum

Radially averaged power spectrum is used to detect the depths of the shallow and deep sources, basement complex, and subsurface geological structures. Many authors have explained the spectral analysis technique (Spector and Grant, 1970; Garcia and Ness, 1994; Tatiana and Angelo, 1998). Fast Fourier transform (FFT) has been applied to RTE magnetic data to calculate the energy spectrum under geosoft environment. The resulted diagrams of the radially averaged power spectrum indicated the average depth levels to the deep and shallow segments (Fig. 12). Depth of the causative body has been determined by calculating slope and then the slope has been used to estimate the depth using the formula $\left[h = \frac{s}{4\pi}\right]$. Power spectrum shows residual anomalies occur at 5 m depth and regional's around 50 m. The profile shows only three slopes from which the above depth has been estimated.

4.2 Euler's deconvolution method

This method is used in the geosoft program, which is based on Euler's homogeneity equation. Euler's homogeneity equation relates the magnetic field and its gradient components to the location of the source. According to Reid et al. (1990) and Thompson (1982), the degree of homogeneity N has been interpreted as a structural index (SI). It is a measure of the rate of change of a magnetic field with distance. Proposed models like contacts are demarcated by the structural index N=0, the magnetic field of a narrow 2-D dyke has a structural index N=1, while a vertical pipe or horizontal cylinder has N=2 and the magnetic sphere has N=3. In the present study, the structural indexes that applied to RTE map are 0, 1, 2, and 3 to select the best solution. RTE magnetic map using SI=0 is shown in Fig. 13a, SI=1 in Fig. 13b, SI=2 in Fig. 13c and SI=3 is shown in Fig. 13d. Structural Index 1 gives better solutions than structural index 0, 2, and 3 because the depth clusters are concentrated linearly at some places in the study area. In the case of SI=0 and SI=3, the data are distributed all over the area and could not make any interpretations pertaining to litho contacts and sphere bodies. Structural Index 2 also shows depth cluster of the Euler solution continuously along the edge of the causative bodies indicates horizontal body. However, the depth clusters are not uniform so it is difficult to conclude as a horizontal cylindrical body. The results are presented in Fig. 13a - Fig. 13d and Table 3.

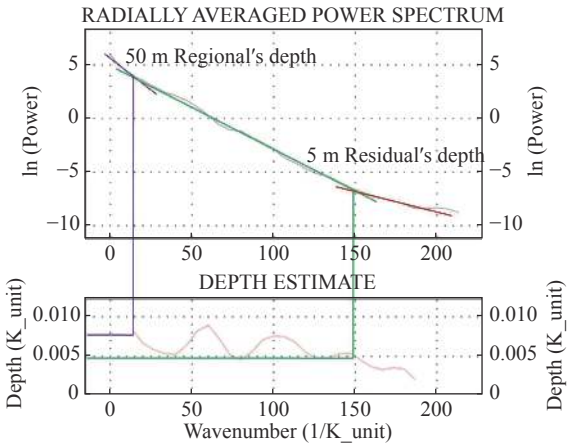

Fig. 12 Depth estimation using radially averaged power spectrum

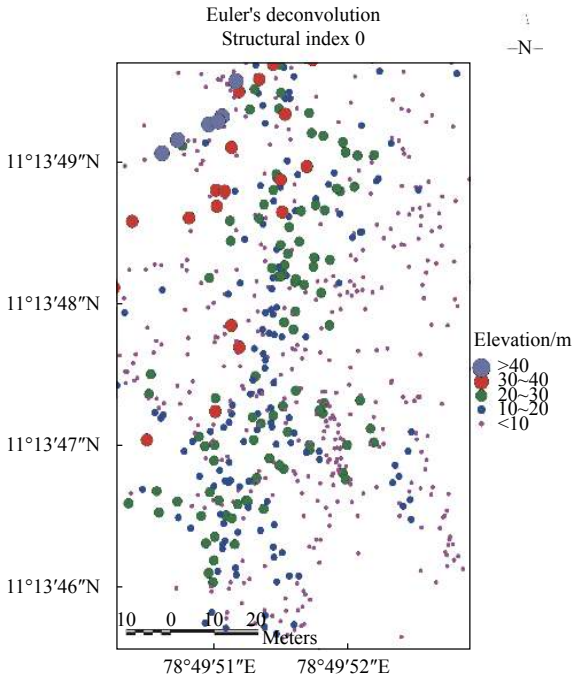

Fig. 13a Depth estimation using structural index 0

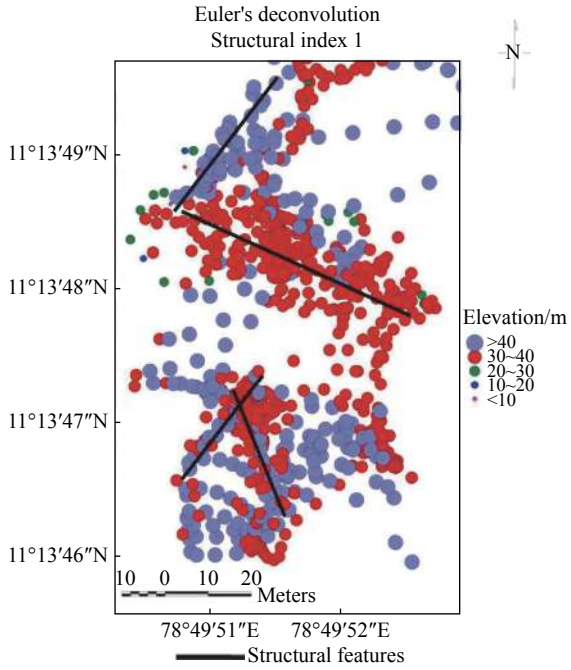

Fig. 13b Depth estimation using structural index 1

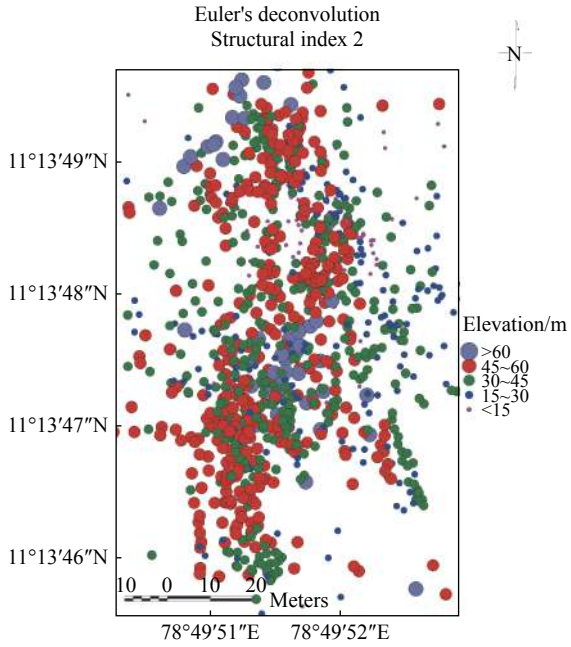

Fig. 13c Depth estimation using structural index 2

5 Conclusions

The objective of this study is to identify suitable sites for open and bore well in the farm and to estimate the depth persistence of those structural elements in the studied area. The most important conclusions reached in this study are following: Two sites were selected and proposed for open and bore well. Circular to semi-circular granitic bodies were mapped using RTE and AS maps. Structural

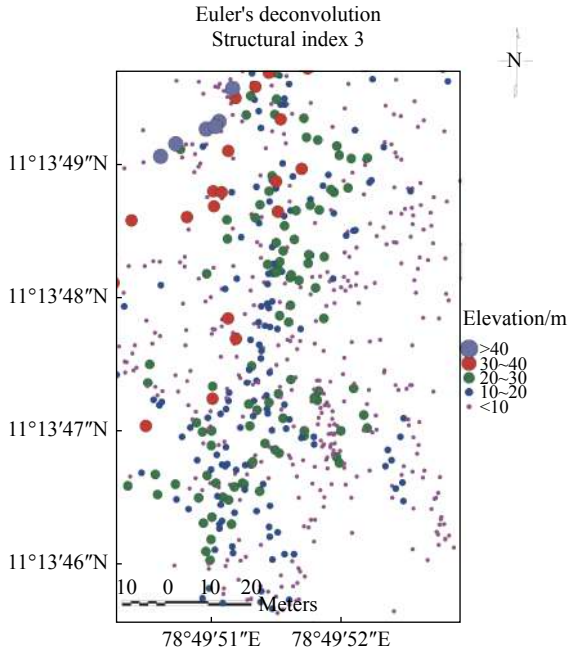

Fig. 13d Depth estimation using structural index 3

elements and directions were established using RTE, TMI and DCF maps. The interpreted subsurface structural elements were oriented into NE-SW and NW-SE directions. Regional and residual anomaly significantly brought out shallow and deep sources. The results of individual profile interpretation of the magnetic field brought to light structurally weak zone between 90 m and 100 m in all the profile lines and sudden decrease of magnetic values from 2 042 nT to 126 nT between 20 m and 30 m in profile line 6 indicate presence of fracture/fault. Radially averaged power spectrum helped to estimate residuals and regional' s depth as 5 m and 50 m, respectively. The Euler deconvolution technique has also been applied for the gridded magnetic to estimate basement depth as well as its structural deformations using structural index 0, 1, 2, and 3. The obtained Euler cluster depths range from <10 m to >90 m. Finally, the result obtained from ground magnetic study could contribute to the understanding of the subsurface structural settings, the depth to the

Table 3 Structural index and depth range using Euler's method

Structural index	Window size	Depth range (m)		Remarks
		Minimum	Maximum	
0	10	0	50	Steps/Contacts
1	10	12	90	2D dyke
2	10	0	70	Vertical pipe/Cylinder
3	10	0	50	Sphere

causative sources and selection of suitable sites for groundwater exploration.

Acknowledgements

The author would like to acknowledge Department of Remote Sensing, Bharathidasan University for the provision of Magnetometer and constant engorgement towards research activities.

References

Adagunodo TA, Sunmonu A, Adeniji A. 2015. An overview of magnetic method in mineral exploration. Journal of Global Ecology and Environment, 3(1): 13-28.

Daniel CU, Chimezie CO, SA Ugwu. 2018. Spectral analysis and euler deconvolution of regional aeromagnetic data to delineate sedimentary thickness in Mmaku Area, South-Eastern Nigeria. An international scientific journal, World Scientific News, 109: 26-42.

Dransfield MH, Buckingham MJ, van Kann FJ. 2018. Lithological Mapping by Correlating Magnetic and Gravity Gradient Airborne Measurements. Journal Exploration Geophysics, 25(1): 25-30.

Garcia JG, Ness GE. 1994. Inversion of the power spectrum from magnetic anomalies. Geophysics, 59: 391-400.

Grant FS, Dodds J. 1972. MAGMAP FFT processing system development notes: Paterson, Grant and Watson Limited.

Hansen RO, Racic L, Grauch VJS. 2005. Magnetic methods in near-surface geophysics. In Near-Surface Geophysics. Society of Exploration Geophysicists Press: 151-175.

Muthamilselvan A, Srimadhi K, Nandhini R, et al. 2017. Spatial confirmation of major lineament and groundwater exploration using ground magnetic method near Mecheri Village, Salem District of Tamil Nadu, India. Journal of Geology & Geophysics, 6(1): 1-10.

MacLeod IN, Jones K, Dai TF. 1993. 3-D analytic signal in the interpretation of total magnetic field data at low magnetic latitudes. Exploration Geophysics, 24(4): 679-688.

Nabighian MN. 1972. The analytic signal of two-dimensional magnetic bodies with polygonal cross-section: Its properties and use for automated anomaly interpretation. Geophysics, 37: 507-517.

Nabighian MN, Grauch VJS, Hansen RO, et al. 2005. The historical development of the magnetic method in exploration. Geophysics, 70: 33-61.

Reid AB, Allsop JM, Granser H, et al. 1990. Magnetic interpretation in three dimensions using Euler Deconvolution. Geophysics, 55: 80-90.

Serguel A Goussev, Jhon W Pierce. 2000. Gravity and magnetic exploration lexicon, acquisition, processing, interpretation and Imaging. Geophysical Exploration & Development Corporation: 1-157.

Spector A, Grant FS. 1970. Statistical models for interpreting aeromagnetic data. Geophysics, 35: 293-302.

Sultan AA. 2015. Integrated geophysical interpretation on the groundwater aquifer (At the North Western Part of Sinai, Egypt). International Journal of Innovative Science, Engineering & Technology, 2(12): 501-522.

Tatiana FQ, Angelo S. 1998. Exploration of a lignite bearing in Northern Ireland, using Maurizio ground magnetic. Geophysics, 62(4): 1143-1150.

Thompson DT. 1982. EULDPH–a new technique for making computer-assisted depth estimates from magnetic data. Geophysics, 47: 31-37.

Tsiboah T. 2002. 2D Resistivity and Time-Domain EM in aquifer mapping: A case study, north of Lake Naivasha, Kenya. Applied Geophysics, ITC. Netherlands: 110.

UNESCO. 1998. Unesco handbook for ground water investigations. Technical report, ITC. Netherlands.